

A 258-year reconstruction of precipitation for southern Northeast China and the northern Korean peninsula

Zhenju Chen^{1,2} · Xingyuan He² · Nicole K. Davi^{3,4} ·
Xianliang Zhang¹

Received: 21 May 2016 / Accepted: 29 August 2016 / Published online: 9 September 2016
© Springer Science+Business Media Dordrecht 2016

Abstract We present a well-verified precipitation reconstruction ($r = 0.612$, $p < 0.01$), spanning 1741 to 1998, for a relatively humid monsoon region from southern Northeast China and the northern Korean peninsula, based on tree rings from Chinese pine and Korean pine. We then investigate the variability of the reconstruction, and identify the leading rainfall patterns and regional dryness and wetness modes during the latest 2.5 centuries. This reconstruction shows that three persistent dry decades occurred during the 1840s, 1910s and 1850s and the three wettest decades occurred during the 1770s, 1820s and 1930s. The five years with lowest rainfall were 1759, 1917, 1841, 1747 and 1839, and 1770, 1938, 1819, 1941 and 1822 were the five years with highest rainfall, respectively. As indicated by the spatial correlation patterns, the reconstruction also exhibits regional characteristics. The variation of reconstructed rainfall significantly corresponds to East Asian monsoon.

1 Introduction

As one of the most significant planetary climate variables, the monsoonal rainfall plays a crucial role in the global climate system and affects roughly half of the world's population (Liu

Electronic supplementary material The online version of this article (doi:10.1007/s10584-016-1796-9) contains supplementary material, which is available to authorized users.

✉ Zhenju Chen
zhenjuchen@hotmail.com

¹ Tree-Ring Laboratory, Forestry College/ Research Station of Liaohe-River Plain Forest Ecosystem CFERN, Shenyang Agricultural University, Shenyang, China

² Qingyuan Forest CERN, Chinese Academy of Sciences, Shenyang, China

³ Tree-Ring Laboratory, Lamont-Doherty Earth Observatory, Columbia University, New York, NY, USA

⁴ Department of Environmental Science, William Paterson University, Wayne, NJ, USA

et al. 2003; Li et al. 2009; Cook et al. 2010). Southern Northeast China and the northern Korean peninsula (hereafter, NCK) are in North East Asia, where water resources depend largely on monsoon precipitation (Li and Zeng 2003; Liu et al. 2003). Also, the general lack of long-term observations of large-scale rainfall variability is a great impediment in Asian monsoon-related moisture studies. It is thus of critical importance to understand the regional monsoonal rainfall patterns as well as their potential driving forces, in order to establish the fundamentals for forecasting droughts and floods.

Recent dendroclimatological studies have been carried out to better understand the effects of climate change on regional ecosystems and to place present climate in a long-term context in NCK (e.g. Shao and Wu 1997; Park et al. 2001; Zhu et al. 2009; Cook et al. 2010; Ohyama et al. 2013). Particularly, substantial effort has been devoted to investigating the variability of past precipitation over Northeast Asia (e.g. Yao et al. 2008; Gao et al. 2014), and some studies have inferred historical variations in precipitation in NCK (e.g., Wada 1910; Jung et al. 2001), especially using proxies like tree-ring (e.g., Liu et al. 2003; Cook et al. 2010; Chen et al. 2011). Particular interest has been given to understand the spatial and temporal variations of extreme rainfall events associated with droughts and floods. However, rainfall-based moisture studies are still very scarce due to the difficulties in modeling the tree radial growth-rainfall relationship in a region with relatively high year-round precipitation (700–1300 mm), and the moisture was also considered as the clearly limiting factor for tree growth in arid regions. Also, the tree-ring based precipitation reconstructions available in this area are focused on specific sites or a small region (e.g., Park et al. 2001; Liu et al. 2003; Chen et al. 2011). Thus, paleoclimatic reconstructions are necessary to develop an understanding of the full range of long-term moisture variability for Northeast Asia.

By coupling instrumental records, historical documents and archives, and combining tree rings of different species from NCK, we demonstrate the fidelity of the model to capture monsoon-related rainfall variability on interannual to centennial timescales, particularly variations in precipitation amplitude. The goals of this study are to: (1) identify the leading rainfall patterns for Northeast Asia, (2) use the tree-ring network to reconstruct regional dryness/wetness modes, and (3) investigate the variability of the reconstruction and explore its linkages with East Asian monsoon.

2 Materials and methods

2.1 Study sites and sample trees

The study region, located in Northeast Asia, includes the southern part of Northeast China, nearly the total area of North Korea, and the northern part of South Korea. This area is characterized by a temperate monsoon climate and complex topography, and about 70 % of the terrain is mountainous (Fig. 1). The region has a southeast–northwest precipitation gradient with increasing rain-shadow effects eastward through the mountain ranges. The driest areas are found near the Qianshan Mountains in China where annual precipitation can drop below 700 mm. Higher precipitation is seen in the Changbai Mountains (ca. 900 mm) and northern South Korea (ca. 1450 mm) (Fig. 1).

Chinese pine (*Pinus tabulaeformis* Carr.) and Korean pine (*Pinus koraiensis* Sied. et Zucc.) are the two main coniferous species in NCK (Xu 1990; Wang et al. 1980). Chinese pine is an endemic conifer in northern China, which occurs naturally in about 12 provinces (Xu 1990), and also in the northern Korea peninsula. The samples were obtained from natural and semi-

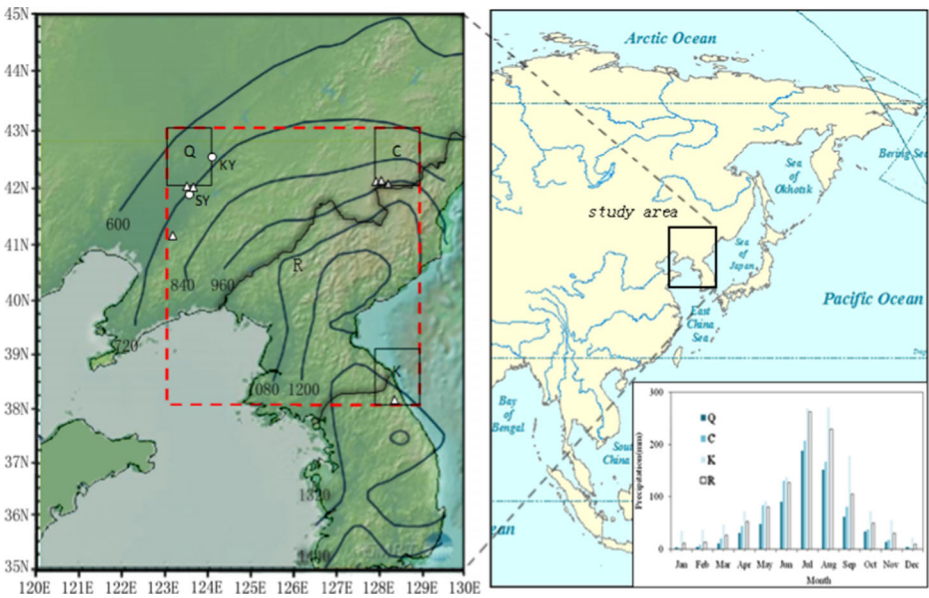


Fig. 1 Map (left) showing the locations of the 7 tree-ring sites (triangles); the 3 CRU TS3.0 $1^\circ \times 1^\circ$ gridpoints of precipitation (rectangle with letter of Q for Qianshan mountains, C for Changbai mountains and K for northern Korea, respectively); and dashed-line rectangle for CRU TS3.0 $5^\circ \times 6^\circ$ gridpoint (R) of precipitation, and the dryness and wetness record stations (circles, Editorial Committee of Academy of Meteorological Science, China Central Meteorological Administration 1981). SY and KY respectively denote Shenyang and Kaiyuan dryness and wetness record station. The contours for the mean October–September averaged CRUTS3.0 precipitation (mm/year) from 1951 to 2006. Lower right plot shows monthly CRU TS3.0 $1^\circ \times 1^\circ$ gridpoint precipitation for Q, C, K and R from 1951 to 2006. The map generates based on Global Multi-Resolution Topography (GMRT) synthesis (Ryan et al. 2009)

natural reserve and preserve areas, which contain old-growth Chinese pine forests located in the Qianshan Mountains and vicinity (Fig. 1). Korean pine, a mountain conifer native to eastern Asia, is the dominant species in the Korean pine-broad leaf mixed forest, and it is the regional climax species of a cool temperate forest (Wang et al. 1980). Our Korean pine samples were obtained from a relatively undisturbed forest in the reserve area on the Changbai Mountains. Data from northern South Korea (Park et al. 2001) were obtained from the International Tree-Ring Data Bank.

2.2 Tree-ring data

A total of 447 increment cores (1–3 per tree) were extracted at breast height from 222 living/dead pines growing on three typical stands across the study area (Fig. 1; Table S1). The majority of samples were collected from high-elevation sites in the mountain ranges (higher than 1000 m a.s.l., except those on/near Qianshan Mountains) (Table S1).

We used dendrochronological techniques (Stokes and Smiley 1968) for new sample processing. The signal free standardized method (Melvin and Briffa 2008) was used for all tree ring series standardization: the indices were computed by ratio during the series processing; negative exponential or linear lines were chose as the curve fit for raw tree-ring measurements detrending in order to preserve as much low-frequency signal as possible; mean chronology calculation used robust Tukey biweight mean; the additional spline variance

stabilization was age depended spline stabilization; the inter-series correlation (r_{Bar}) window width for variance stabilization was 31 years as well as the expressed population signal (EPS) with a threshold value of 0.85 (Wigley et al. 1984); the signal free convergence test based on minimizing the mean absolute difference between the current and proceeding chronologies.

The tree-ring indices were finally averaged together to generate a Standard chronology for each site using the program RCSsigFree v45 (<http://www.ldeo.columbia.edu/tree-ring-laboratory/resources/software>). Thereafter, the Standard chronologies for seven sites across southern NCK, were developed (Fig. 2; Table S1). Based on the well agreement of Qianshan chronologies and Changbai chronologies (Table S1; S2), we respectively combined the raw tree-ring measurements from Changbai Mountains and Qianshan Mountains, and developed a composite Standard chronology for Changbai Mountains and one for Qianshan Mountains. A general Standard chronology for the whole study area were also developed by combing the raw tree-ring measurements from Changbai Mountains, Qianshan Mountains and northern South Korea (Fig. 2d).

2.3 Climate data

Meteorological records in Northeast Asia are very scarce, particularly in the northern Korean peninsula; and out of 22 stations in China in the NCK, only one extends back to 1951 and four extend back 1952. Also, the merging CRU TS3.0 data has lower random and higher spatial (regional) consistence as compared to the individual meteorological data for regional climate variation and regional growth-climate response assessment. We therefore chose to use spatially interpolated meteorological data from CRU TS3.0 global $1^\circ \times 1^\circ$ gridded meteorological datasets nearest to the sample sites from 1953 to present, to investigate growth - climate relationships for NCK.

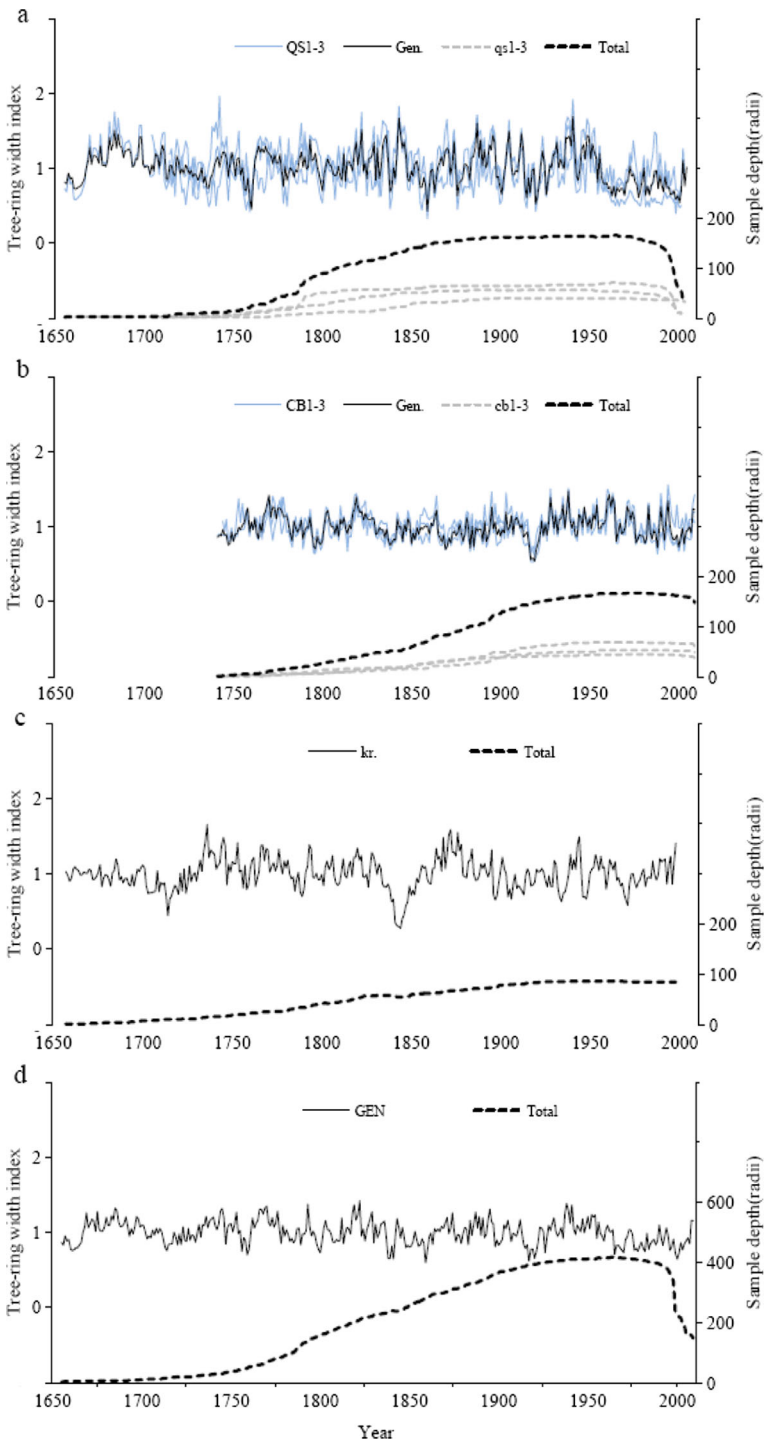
The averaged precipitation and temperature data from the area $5^\circ_{\text{Latitude}} \times 6^\circ_{\text{Longitude}}$ ($38^\circ\text{--}43^\circ\text{N}$, $123^\circ\text{--}129^\circ\text{E}$) covers all the tree-ring sampling sites from 1953 to 2006. The data for the gridpoints near the Qianshan Mountains ($42^\circ\text{--}43^\circ\text{N}$, $123^\circ\text{--}124^\circ\text{E}$), Changbai Mountains ($42^\circ\text{--}43^\circ\text{N}$, $128^\circ\text{--}129^\circ\text{E}$) and northern South Korea ($38^\circ\text{--}39^\circ\text{N}$, $128^\circ\text{--}129^\circ\text{E}$) sample sites were used as local meteorological records to test the affected significance of local climate and the corresponding chronology. The correlations are significant ($p < 0.05$) between the averaged precipitation and temperature data in the grids and at the stations.

The East Asian monsoon index (Li and Zeng 2002; 2003), a spatial reconstruction of PDSI for NCK (Cook et al. 2010) (data of gridpiont of $41^\circ15'\text{N}$ $123^\circ45'\text{E}$, $41^\circ45'\text{N}$ $126^\circ15'\text{E}$ and their average), and the Korean seasonal rainfall records from 1777 to 1907 based on an ancient rain-measuring device (Wada 1910; Jung et al. 2001), were used for comparison.

2.4 Historical documents and archives

The 120-station discontinuous dryness/wetness records over China from China Meteorological Data Sharing System (<http://cdc.cma.gov.cn/home.do>) [developed by Editorial Committee of Academy of Meteorological Science, China Central Meteorological Administration

Fig. 2 Standard chronologies and the corresponding sample size. QS1–3, CB1–3 indicate individual Standard chronologies, respectively (refer to Table S1), and their corresponding sample depths qs1–3, cb1–3; Gen is composite chronology derived from all samples of QS1, QS2 and QS3 in (a) and CB1, CB2, CB3 in (b), and Jkr is Standard chronology for northern Korea (c); Total is total sample depth in (a) - (d); GEN is the general Standard chronology based on all samples (d)



(AMSCCMA, 1981], which were often used in China's dry/wet assessment (e.g., Shen et al. 2007; Chen et al. 2011), and the groundwater records in the Liaoning province, China in NCK (Liaoning Water Resource Bulletin 1991–1998) were used as the main historical documents and archives to compare with our reconstruction.

Specifically, the 120-station discontinuous dryness/wetness records (AMSCCMA 1981) were developed into a general moisture variable time series of China (*DWR*) for specific comparison based on the calculation of $DWR_i = \text{Log}[(DR_i/WR_i)/(N_i/120)]$. Where DWR_i is dryness and wetness index at year i ; DR_i , WR_i and N_i , respectively, represents the number of available dryness and weak dryness records, the number of available wetness and weak wetness records and the total number of available dry and wet records across China (120 stations) at year i . $DWR_i > 0$, $DWR_i < 0$ or $DWR_i = 0$ respectively represents a generally dry, wet and normal moisture condition in year i across China.

2.5 Statistical analysis

Climate-growth relationships were investigated by correlating ring-width indices with monthly and seasonal climate data for two calendar years when both meteorological records and tree-ring data are available (1953–1998). Precipitation derived dryness/wetness assessments were based on the method of AMSCCMA (1981).

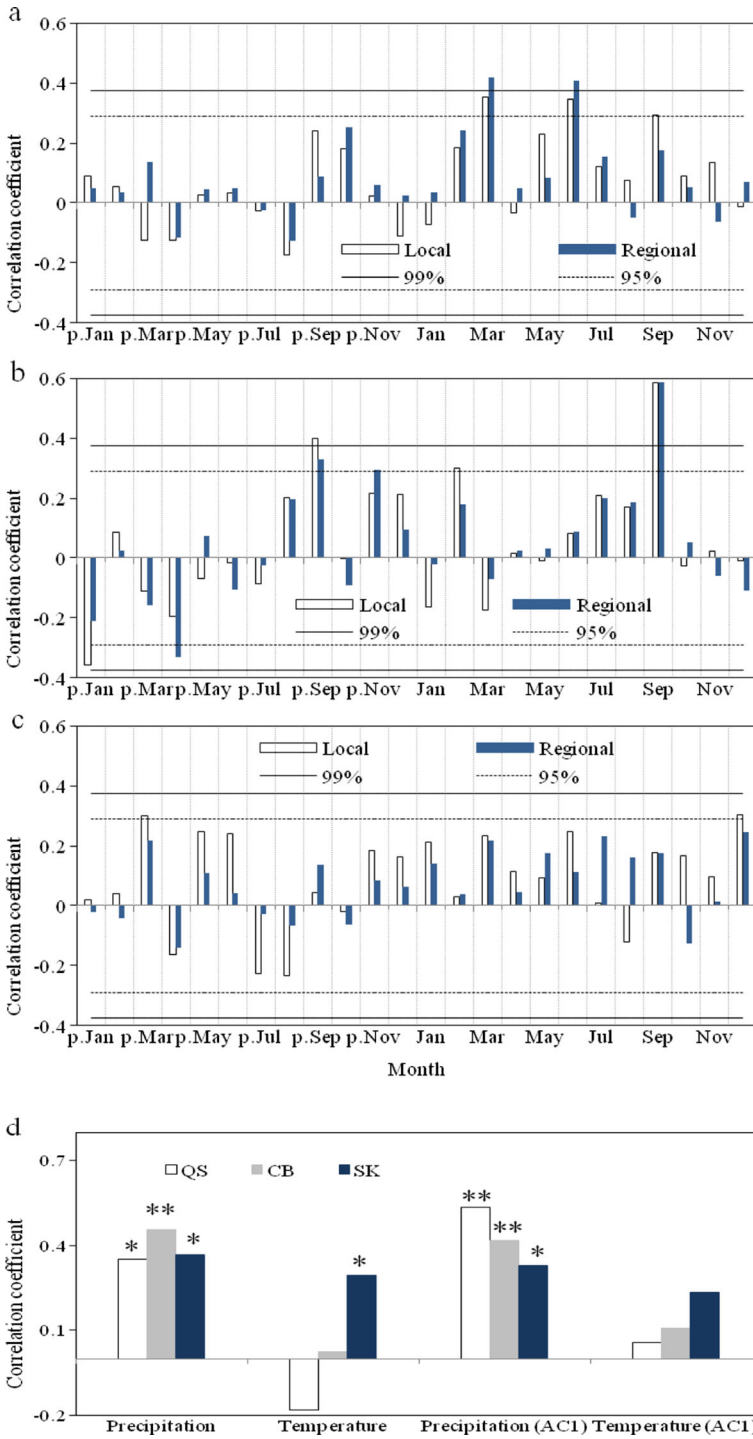
The statistical fidelity of the model was examined by split sample calibration-verification tests (Meko and Graybill 1995). Spatial correlation analyses were performed using the KNMI Climate Explorer (<http://www.knmi.nl>).

3 Results

3.1 Chosen season for reconstruction

Our tree-ring width shows better relationships with precipitation compared to temperature, particularly the low correlations with seasonal temperature, e.g., in October–April (Fig. 3d; S1). Specifically, the tree rings from Korean pine from Changbai Mountains had higher positive correlations with winter and summer precipitation (Fig. 3); radial growth of Chinese pine was positively affected by monthly precipitation in February–September; and the tree ring widths from the Korean pine site of northern South Korea were positively correlated to precipitation in November–June (Fig. 3). However, the pine's local and regional climate-radial growth response is consistent, demonstrating homogeneous macro-scale climatology affecting all sites.

Fig. 3 Correlations of tree-ring widths with precipitation (a–c) and regional October–September precipitation/temperature (d). Local denotes the correlations of tree rings from Qianshan mountains (a), Changbai mountains (b) and northern Korea (c) with CRU TS3.0 $1^\circ \times 1^\circ$ gridpoint of precipitation for area of Q, C and K (refer to Fig. 1); Regional denotes the correlations of tree rings from Qianshan mountains (a), Changbai mountains (b) and northern Korea (c) with CRU TS3.0 $1^\circ \times 1^\circ$ gridpoint of precipitation for area of $5^\circ \times 6^\circ$ (refer to Fig. 1). The black dashed lines and “*” are the 95 % confidence limits, and the black solid lines and “***” are the 99 % confidence limits. “p.” denotes the prior year; QS, CB and SK respectively is the general Standard chronology of Qianshan Mountains, the general Standard chronology of Changbai Mountains and the Standard chronology of northern South Korea; AC1 denotes the first-difference variables



The highest correlations between tree rings and the seasonalized precipitation were from prior October to current September (hereafter denoted as “October–September” for convenience) from 1953 to 1998 (Fig. 3), particularly the coherence of their high frequency signals between tree radial growth and climate change in this large area of mountainous terrain, e.g., the higher correlations between their first-difference variables. Therefore October–September was chosen as the season for precipitation reconstruction.

3.2 Reconstruction results

Besides the general Standard chronology based model, the models based on simple averaging, first principal component, first and second principal component, and total of three regional Standard chronologies were also investigated, and that the significant and reliable results were found in all regressions (Table S3). For convenience, the remaining discussions in this paper will mainly focus on the reconstruction based on the general Standard chronology using simple linear regressions (Fig. 4).

There is a highly significant relationship between actual and estimated precipitation over the full 1953–1998 period ($r = 0.612$, $p < 0.001$). The overall split calibration-verification tests indicate a reasonable level of validity for our regression model (Table 1): the reduction of error (RE) and the coefficient of efficiency (CE) tests of split sample calibration-verification tests are all positive.

The reconstruction generally is an average level of the regional precipitation for the area on a $5^{\circ}_{\text{Latitude}} \times 6^{\circ}_{\text{Longitude}}$ (Fig. 1) scale and has a mean of 1011.6 mm. The maximum difference of mean annual precipitation in NCK is ca.612 mm (the upper limit is ca.1283 mm near northern South Korea and the lower limit is ca.671 mm around Qianshan Mountains), and about 71.3 % (184 years) of the total 258 years from 1741 to 1998 are in the precipitation range of 1000 ± 100 mm across the entire region (Fig. 4). Here, the maximum and minimum precipitation region respectively denotes as the southeastern and northwestern part of the study area, and the correlation coefficient of the maximum and minimum precipitation with the average data of whole study area respectively is 0.546 and 0.670 ($p < 0.01$).

3.3 Dry/wet periods

In general, a pluvial occurs around the 1770s lasting 11 years; another wet period occurs ca.1820, with a sharp decline in precipitation from 1820s–1840s; the lowest precipitation period occurred near 1920, increase until the early 1940s, and sharply declines until 1998. Specifically, 1759, 1917, 1841, 1747 and 1839 were the five driest rainfall years, and 1770, 1938, 1819, 1941 and 1822 were the five wettest rainfall years, respectively; the 1840s, 1910s and 1850s were the three driest decades, the 1770s, 1820s and 1930s were the three wettest decades, respectively; 1850–1899 and 1950–1998 were the wettest and the driest half-centuries, respectively; and the twentieth century was slightly drier than the nineteenth century. In addition, based on the results of October–September precipitation derived dryness/wetness index, there were 90 wet years, 97 dry years and 70 normal years over the whole period.

After applying a 10-year low pass filter to the October–September precipitation, we identified 10 relatively wet periods and 10 relatively dry periods for the past dry/wet conditions in this region (Fig. 4). Here, for a wet/dry period, the October–September precipitation must be lower/higher than the average of October–September precipitation for the period 1741–1998 and the wetness/dryness must continue for at least 5 years. The periods 1765–1780, 1815–

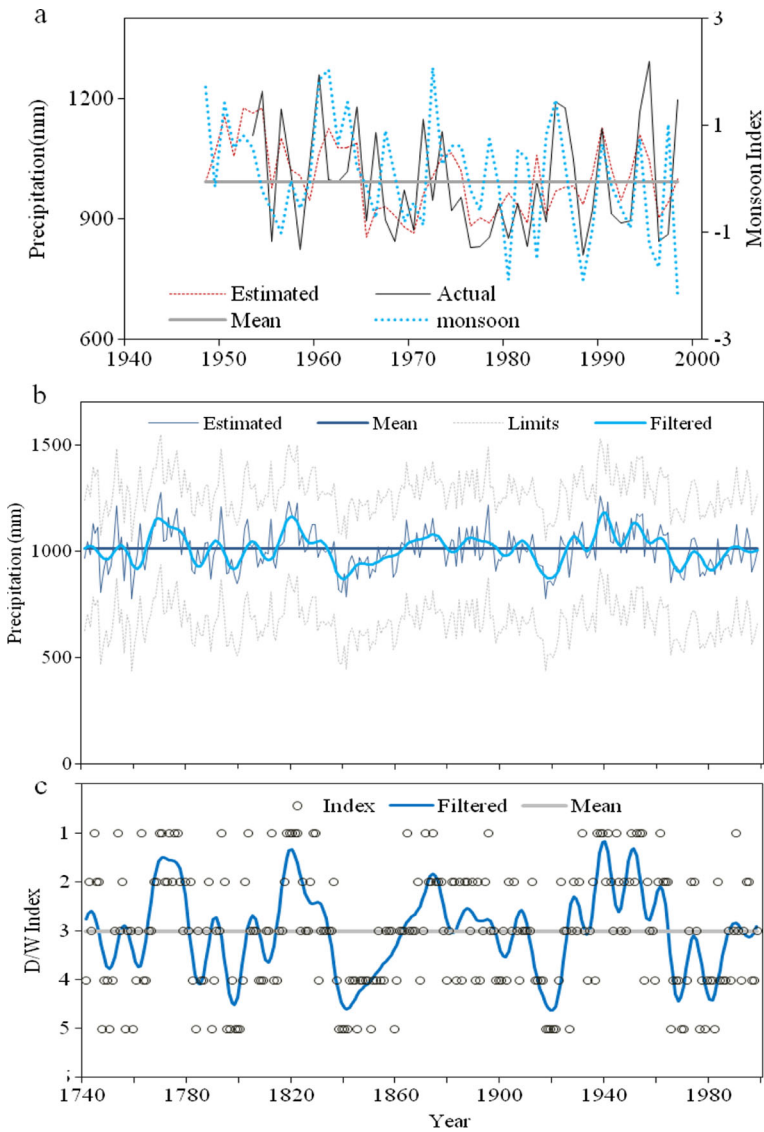


Fig. 4 The comparison between the actual, reconstructed October–September precipitation and East Asia monsoon index (<http://web.lasg.ac.cn/staff/ljp/data-monsoon/EASMI.htm#The> EASM index data) (Li and Zeng 2002; 2003) (a) during the common period of 1953–1998 and 1950–1998 respectively, and the reconstructed annual rainfall (b) and dryness and wetness (D/W Index) data (c) using the Standard chronologies from 1741 to 1998. For D/W Index, 1 indicates wetness (34 yrs., 13.2 %), 2 indicates weak wetness (56 yrs., 21.7 %), 3 indicates normal status (70 yrs., 27.1 %), 4 indicates weak dryness (67 yrs., 26.0 %) and 5 indicates dryness (30 yrs., 11.6 %). Precipitation is expressed as anomalies with respect to the 1953–1998 average: in the (b) panel, the thin solid curve is the annually reconstructed precipitation, the thin dashed curves are the top (estimates + 271.0 mm) and bottom (estimates - 340.6 mm) limits of regional rainfall based on maximum and minimum CRU TS3.0 1° × 1° gridded (local) precipitation records of the study area (5° × 6° gridpoint), the thick grey line respectively indicates average of actual data in 1953–1998 (a) and the reconstructions (b and c) in the whole period, the thick curve respectively indicates the smoothed data employing an 10-year low-pass filtered method (b and c), and circles indicate D/W Index based on the method of AMSCMA (1981)

Table 1 Statistics of calibration and verification test results for the common periods

	Calibration	Verification	Calibration	Verification	Final calibration
	1953 ~ 1975	1976 ~ 1998	1976 ~ 1998	1953 ~ 1975	1953 ~ 1998
<i>r</i>	0.578 (0.683)	0.646 (0.678)	0.646 (0.678)	0.578 (0.683)	0.612 (0.681)
<i>R</i> ²	0.334	0.417	0.417	0.334	0.375 (0.464)
adjusted <i>R</i> ²	0.302		0.389		0.361 (0.451)
<i>RE</i>	0.334 (0.400)	0.412 (0.441)	0.417 (0.458)	0.238 (0.471)	
<i>CE</i>	0.334 (0.400)	0.352 (0.435)	0.417 (0.458)	0.135 (0.465)	
<i>t</i> -stat	3.277**(2.898**)	2.447* (3.185**)	3.345**(3.182**)	1.812* (2.916*)	

* and **respectively indicates significant at $p < 0.05$ and $p < 0.01$; the statistics with parentheses are for first difference results. RE is reduction of error statistic and CE is coefficient of efficiency statistic

1833, 1863–1879, 1884–1898 and 1934–1963 were the wettest, and 1834–1862, 1911–1925 and 1964–1987 were the driest to exceed 10 years.

3.4 Relationship between reconstruction and east Asian summer monsoon

The reconstructed rainfall significantly correlates with the East Asian summer monsoon index ($r_{\text{June}} = 0.291$, $r_{\text{June to August}} = 0.288$, $p < 0.05$), especially in June, the junction of the spring and summer of study area during the common periods of 1948–1998, implying the importance of occurrence and strength of East Asian summer monsoon to regional moisture variation and tree growth.

4 Discussions

4.1 Rainfall–growth relationships

Annual growth from Korean pine exhibit a strong temperature signal and were therefore used to reconstruct temperatures (Shao and Wu 1997; Park et al. 2001; Zhu et al. 2009; Ohyama et al. 2013). Because of elevation and humidity, precipitation was previously considered to have a less significant effect on the radial growth of the two species than temperature, especially those in the Changbai Mountains and northern South Korea. Since we find weak relationships with our data and temperature (Fig. 3; S1) and previous studies allow for a relatively detailed understanding of the long-term trends and variation in regional temperatures, and potential effects of temperature change on radial growth of local trees over the past several hundred years or more (Shao and Wu 1997; Park et al. 2001; Zhu et al. 2009; Ohyama et al. 2013), further discussion is warranted for precipitation effects on local trees.

Chinese pine in NCK is at the northeastern boundary of its natural distribution and is in a drier site compared to the Korean pine site. Korean pine naturally occurs in a region of NCK, and this species show gradual vulnerability to available water supply in this area (Wang et al. 1980). Specifically, the radial growth of Korean pine shows a decreasing climatic sensitivity to an increase in precipitation, as seen in the decreasing correlations between tree radial growth and precipitation from low-rainfall region to high-rainfall region (Fig. 3d).

Radial growth of trees from different sites shows slightly different responses to regional and local rainfall variation. First of all, winter-spring precipitation seems crucial for tree radial growth in the growing season (Shi et al. 2008), and the main water source in winter comes from snow in NCK. On the other hand, the relatively high correlations of the precipitation in June in Qianshan Mountains and in September in Changbai Mountains with their chronologies suggest that trees are more sensitive to moisture deficiency in the growing season in lower rainfall region of NCK. Even though sufficient precipitation or humidity reduced the sensitivity of trees to moisture variation in NCK, precipitation, like temperature can also be defined as one of main factors to radial growth of trees as the year-round and critical seasonal rainfall shows significant effects on tree radial growth.

4.2 Rainfall related dryness and wetness assessment

During the last 250 years, this region seems to be characterized by a rather “stable” or “even” precipitation regime, since the reconstructed precipitation patterns varies around 1000 mm (Fig. 4b) with no significant trends across the entire time period - and lowest values at 800 mm and the highest values at 1200 mm.

Specifically, coinciding with the longest and driest period of 1832–1864 in our reconstruction, an extreme low-growth period of pines existed in the 1830s–1860s particularly in northern South Korea (Fig. 2, 4). A corresponding significant decrease ($p < 0.05$) was found in historical Korean seasonal rainfall records (Wada 1910; Jung et al. 2001) during the interval of 1832–1864, and more than 70 % of the records in 1834–1844 are below the average of the total records from 1777 to 1907 in South Korea (Fig. S2). The reconstructed dry interval of 1832–1864, sustained climate extremes (drought in north or floods in south) were also detected across China (AMSCMA 1981; Liu et al. 2010; Li et al. 2009; Cook et al. 2010), Mongolia (Davi et al. 2006; Li et al. 2009), Korea (Wada 1910; Jung et al. 2001; Liu et al. 2003; Cook et al. 2010) and Southeast Asia (Buckley et al. 2010; Cook et al. 2010).

The longest wet period, 1934–1963, coincided with findings from East China where there was severe flooding along the Yangtze River in 1935 and 1954 (Wang et al. 2004). Likewise, the severe floods along the Yangtze River in 1870 and 1931, respectively, corresponded to our wet periods from 1863 to 1879 and 1926–1931. In addition, the annual amount of groundwater in the Liaoning province in NCK (Liaoning Water Resource Bulletin 1991–1998), is significantly correlated to October–September precipitation ($r_{1991-1998} = 0.754$, $p < 0.05$), since the regional water resource deficits were dominated by the regional precipitation pattern, suggesting a long-term sharp drop in the October–September precipitation from the 1950s to 1990s.

The reconstructed precipitation variations show spatial and temporal homogeneity across study area and vicinity, but generally heterogeneity at a larger scale, suggesting a strong rainfall heterogeneity in northeastern Asia (Fig. 5). The year-round rainfall estimates for NCK and archive-based dryness/wetness assessment for China indicate a slightly higher moisture condition during 19th than that of twentieth century. However, the nineteenth century was a relatively dry period in general as compared to the twentieth century in northwestern China, Pakistan and Mongolia (AMSCMA 1981; Pederson et al. 2001; Davi et al. 2006; Treydte et al. 2006; Cook et al. 2010), and even in Western North America (Cook et al., 2004). The different atmospheric circulation regimes were considered the main cause of this spatial-temporal heterogeneity (Treydte et al. 2006). It is still difficult to clarify the connections, mechanisms and drivers of these contemporaneous global-scale rainfall fluctuations across the

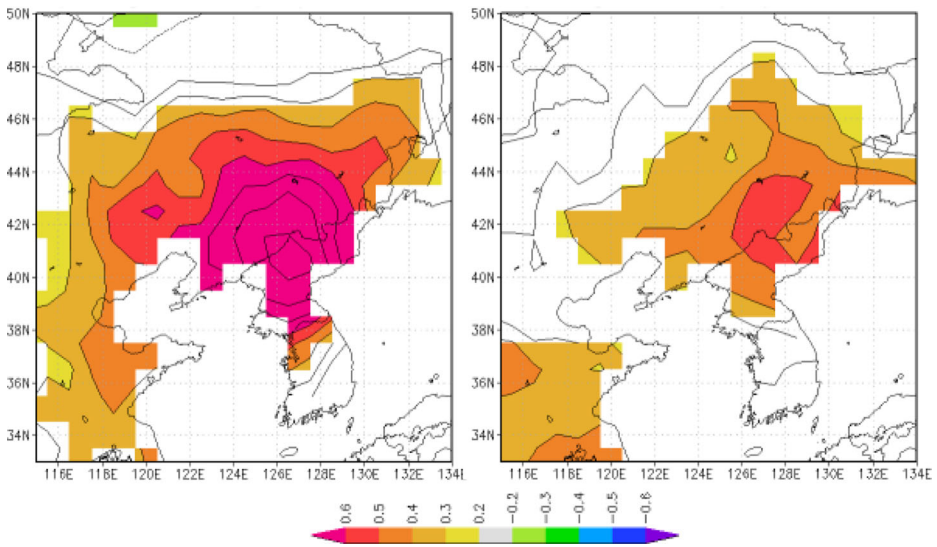


Fig. 5 Correlation patterns of actual (*left*) and reconstructed (*right*) rainfall with the concurrent CRU TS3.0 1° × 1° gridpoint rainfall over their overlapping periods (October–September, 1953–1998)

Northern Hemisphere, which requires further investigation. Consistent with other findings (Li et al. 2009; Cook et al. 2010; Liu et al. 2010; Chen et al. 2011), our reconstructed and instrumental data show severe moisture deficit that have decreased significantly over northeast Asia since the mid-1950s (e.g. 1964–1987 and 1993–1998). Recent long-term trend towards dry condition is consistent with or related to temperature increase of the region and the globe (Treydte et al. 2006). Severe droughts and dry decades like 1859 and the 1920s (particularly 1920, 1922 and 1926) at inter-annual and decadal time scales, were clearly recorded in our work (Fig. 4) as well as many other tree-ring series and precipitation records in China (e.g., Wang et al. 2004; Liang et al. 2007).

4.3 Linkages to east Asian monsoon

The East Asian monsoon climate regimes dominate the regional deficit and abundance of water availability and variability of temperature, e.g., the annual dry season is associated with weaker summer East Asian monsoon events ($p < 0.05$) (Fig. 4) and cold winters are related to stronger winter East Asian monsoon climate (Li et al. 2009; Zhu et al. 2009). The decreasing October–September precipitation during the late 1900s is consistent with documented moisture data in Korea, northern China, and Mongolia (Liu et al. 2003; Li et al. 2009; Chen et al. 2011), which indicates a persistent weakening of the Asia monsoon climate since the 1960s, especially after the 1970s, and also supports the findings: a dry monsoon (after 1958) (Fu and Fletcher 1988; Liu et al. 2003).

Our tree-ring based precipitation shows more significant correlations with the East Asian monsoon index than that of instrumental precipitation records, which might be due to the tree-ring data being a composite of multiple environmental variables. The correlation between the East Asian summer monsoon index (Li and Zeng 2002; 2003) and our reconstructed year-round precipitation is higher ($r = 0.288$, $p < 0.05$) than that of the reconstructed seasonal PDSI data ($r = -0.045$, $p = 0.750$) (Cook et al. 2010) during the common period (1948–1998).

Some deviations of dry/wet phases also exist between the reconstructed PDSI data for NCK and our reconstruction, e.g., the 1810s–1830s, 1830s–1860s, and 1910s–1920s (Fig. S2), particularly the “Great Drought” (1876–1878), which affected NCK (Cook et al. 2010). Likewise, large parts of eastern China experienced severe drought from 1876 to 1878, and nearly half the dryness/wetness records (AMSCCMA 1981) showed dry condition across China at that time (41 % in 1876, 54 % in 1877 and 36 % in 1878). However, a generally normal moisture condition without severe drought is shown by our reconstruction as well as the local archive from Shenyang and Kaiyuan (Fig. 1) at that time: weak dryness in 1876, normal moisture condition in 1877, and normal moisture condition in the former and weak wetness in the latter in 1878. The drought decreases from south to north and from plains to mountain areas across the study area in China (AMSCCMA 1981; Zhang and Liang 2010). In addition, the historical Korean rainfall records only record a low rainfall year in 1876 during 1875–1879 (below the average of 1777–1907, when the traditional Korean rain gauge was used) (Wada 1910; Jung et al. 2001).

The NCK’s northern edge is at the transition zone of subtropical monsoon system and the temperate frigid monsoon system (Li and Zeng 2003). Interactions between the rapidly mixing atmosphere and the slowly changing oceans are largely responsible for the monsoon season in East Asia, particularly as they affect NCK. Specifically, the monsoon front approaches the southern part of the NCK- Korean Peninsula in late June, migrating gradually to the north (Ding and Chan 2005), and then significant rainfall occurs when a stationary front lies over this region. Therefore, the drought in the southern part of NCK may not always occur simultaneously with that in northern and eastern China (Zhang and Liang 2010).

Acknowledgments This work was funded by the National Natural Science Foundation of China Project 41271066, 31570632, 41571094 and 41601045, and the US National Science Foundation Project AGS-PRF: #1137729. Dr. Steve W. Leavitt helped to improve this work. We thank contributors of Korean tree-ring data.

References

- Buckley BM, Anchukaitis KJ, Penny D, Fletcher R, Cook ER, Sano M, Nam L, Wichienkeo A, Minh TT, Hong TM (2010) Climate as a contributing factor in the demise of Angkor, Cambodia. *PNAS* 107:6748–6752. doi:10.1073/pnas.0910827107
- Chen Z, He X, Cook ER, He H-S, Chen W, Sun Y, Cui M (2011) Detecting dryness and wetness signals from tree rings in Shenyang, Northeast China. *Palaeogeogr Palaeoclimatol Palaeoecol* 302:301–310. doi:10.1016/j.palaeo.2011.01.018
- Cook ER, Woodhouse C, Eakin CM, Meko DM, Stahle DW (2004) Long-Term Aridity Changes in the Western United States. *Science* 306(5698):1015–1018
- Cook ER, Anchukaitis KJ, Buckley BM, D’Arrigo RD, Jacoby GC, Wright WE (2010) Asian monsoon failure and megadrought during the last millennium. *Science* 328:486–489. doi:10.1126/science.1185188
- Davi NK, Jacoby GC, Curtis AE, Baatarbileg N (2006) Extension of drought records for Central Asia using tree rings: west-Central Mongolia. *J Clim* 19:288–299
- Ding Y, Chan JCL (2005) The east Asian summer monsoon: an overview. *Meteorog Atmos Phys* 89:117–142. doi:10.1007/s00703-005-0125-z
- Editorial Committee of Academy of Meteorological Science, China Central Meteorological Administration (1981) Yearly charts of dryness/wetness in China for the last 500-year period (in Chinese). Map Publishers, Beijing
- Fu CB, Fletcher J (1988) Large signal of climatic variation over the ocean in the Asian monsoon region. *Adv Atmos Sci* 5:389–404

- Gao Z, Hu Z-Z, Zhu J, Yang S, Zhang R-H, Xiao Z, Jha B (2014) Variability of summer rainfall in Northeast China and its connection with spring rainfall variability in the Huang-Huai region and Indian Ocean SST. *J Clim* 27:7086–7101. doi:[10.1175/JCLI-D-14-00217.1](https://doi.org/10.1175/JCLI-D-14-00217.1)
- Jung H-S, Lim G-H, Oh J-H (2001) Interpretation of the transient variations in the time series of precipitation amounts in Seoul, Korea. Part I: diurnal variation. *J Clim* 14:2989–3004
- Li J, Cook ER, Chen F, Davi N, D'Arrigo R, Gou X, Wright WE, Fang K, Jin L, Shi J, Yang T (2009) Summer monsoon moisture variability over China and Mongolia during the past four centuries. *Geophys Res Lett* 36: L22705. doi:[10.1029/2009GL041162](https://doi.org/10.1029/2009GL041162)
- Li J, Zeng Q (2002) A unified monsoon index. *Geophys Res Lett* 29(8):1274. doi:[10.1029/2001GL013874](https://doi.org/10.1029/2001GL013874)
- Li J, Zeng Q (2003) A new monsoon index and the geographical distribution of the global monsoons. *Adv Atmos Sci* 20:299–302
- Liang EY, Shao XM, Liu HY, Eckstein D (2007) Tree-ring based PDSI reconstruction since AD 1842 in the Ordindag sand land, East Inner Mongolia. *Chin Sci Bull* 52(19):2715–2721
- Liu Y, Park W-K, Cai Q, Seo J-W, Sook J-H (2003) Monsoonal precipitation variation in the East Asia since A.D. 1840—Tree-ring evidences from China and Korea. *Sci China Ser D* 46:1031–1039
- Liu Y, Tian H, Song H, Liang J (2010) Tree ring precipitation reconstruction in the Chifeng-Weichang region, China, and east Asian summer monsoon variation since a.D. 1777. *J Geophys Res* 115:1–9. doi:[10.1029/2009JD012330](https://doi.org/10.1029/2009JD012330)
- Meko DM, Graybill DA (1995) Tree-ring reconstruction of upper Gila River discharge. *Water Resour Bull* 31: 605–616
- Melvin TM, Briffa KR (2008) A “signal-free” approach to dendroclimatic standardisation. *Dendrochronologia* 26:71–86
- Ohyama M, Yonenobu H, Choi J-N, Park W-K, Hanzawa M, Suzuki M (2013) Reconstruction of Northeast Asia spring temperature 1784–1990. *Clim Past* 9:261–266
- Park W-K, Seo J-W, Kim Y, Oh J-H (2001) July–August temperature of central Korea since 1700 AD: reconstruction from tree-rings of Korean pine (*Pinus koraiensis*). *Palaeobotanist* 50:107–111
- Pederson N, Jacoby GC, D'Arrigo R, Cook ER, Buckley BM, Dugarjav C, Mijiddorj R (2001) Hydrometeorological reconstructions for northeastern Mongolia derived from tree rings: AD 1651–1995. *J Clim* 14:872–881
- Ryan WBF, Carbotte SM, Coplan JO, O'Hara S, Melkonian A, Arko R, Weissel RA, Ferrini V, Goodwillie A, Nitsche F, Bonczkowski J, Zensky R (2009) Global multi-resolution topography synthesis. *Geochem Geophys Geosyst* 10:Q03014. doi:[10.1029/2008GC002332](https://doi.org/10.1029/2008GC002332)
- Shao XM, Wu XD (1997) Reconstruction of climate change on Changbai Mountain, Northeast China using tree-ring data (in Chinese). *Quaternary Sci* 1:76–85
- Shen C, Wang W-C, Hao Z, Gong W (2007) Exceptional drought events over eastern China during the last five centuries. *Clim Chang* 85:453–471
- Shi JF, Liu Y, Vaganov EA, Li JB, Cai QF (2008) Statistical and process-based modeling analyses of tree growth response to climate in semi-arid area of north Central China: a case study of *Pinus tabulaeformis*. *J Geophys Res* 113:G01026. doi:[10.1029/2007JG000547](https://doi.org/10.1029/2007JG000547)
- Stokes MA, Smiley TL (1968) *An Introduction to Tree Ring Dating*. The University of Chicago Press, Chicago
- Treydte K, Schleser GH, Helle G, Winiger M, Frank DC, Haug GH, Esper J (2006) The twentieth century was the wettest period in northern Pakistan over the past millennium. *Nature* 440:1179–1182
- Wada Y (1910) *Scientific memoirs of the Korean meteorological observatory, vol 1*. Chemulpo, Korea (In Japanese and French)
- Wang Z, Xu ZB, Li X (1980) The main forest types and their features of community structure in northern slope of Changbai Mountain (in Chinese). *Res Forest Ecosyst* 1:25–32
- Wang S, Zhu J, Cai J (2004) Interdecadal variability of temperature and precipitation in China since 1880. *Adv Atmos Sci* 21(3):307–313
- Wigley T, Briffa KR, Jones PD (1984) On the average value of correlated time series, with applications in dendroclimatology and hydrometeorology. *J Appl Meteorol Climatol* 23:201–213
- Xu HC (1990) *Pinus tabulaeformis* (in Chinese). China Forestry Press, Beijing, pp. 18–23
- Yao C, Yang S, Qian W, Lin Z, Wen M (2008) Regional summer precipitation events in Asia and their changes in the past decades. *J Geophys Res Atmos* 113(D17107):1–17. doi:[10.1029/2007JD009603](https://doi.org/10.1029/2007JD009603)
- Zhang D, Liang Y (2010) A long lasting and extensive drought event over China during 1876–1878. *Adv Clim Chang Res* 6(2):106–112
- Zhu HF, Wang XQ, Shao XM, Yin ZY (2009) Tree ring-based February–April temperature reconstruction for Changbai Mountain in Northeast China and its implication for east Asian winter monsoon. *Clim Past* 5:1–6